Vaccination of SARS-CoV-2-infected individuals expands a broad range of clonally diverse affinity-matured B cell lineages

Mark Chernyshev
Department of Microbiology, Tumor and Cell Biology, Karolinska Institutet https://orcid.org/0000-0003-1622-9240

Mrunal Sakharkar
Adimab LLC

Ruth Connor
Dartmouth College

Haley Dugan
Adimab LLC

Daniel Sheward
Karolinska Institutet https://orcid.org/0000-0002-0227-5636

C. Garrett Rappazzo
Adimab LLC

Aron Stålmarck
Department of Microbiology, Tumor and Cell Biology, Karolinska Institutet https://orcid.org/0000-0002-2632-6266

Mattias Forsell
Umeå University https://orcid.org/0000-0001-6904-742X

Peter Wright
Department of Pediatrics, Dartmouth-Hitchcock Medical Center

Martin Corcoran
Karolinska Institute

Ben Murrell
Karolinska Institutet https://orcid.org/0000-0002-0393-4445

Laura Walker
Invivyd Inc.

Gunilla Karlsson Hedestam (gunilla.karlsson.hedestam@ki.se)
Karolinska Institute

Article

Keywords: SARS-CoV-2, HCoV, vaccination, monoclonal antibodies, neutralization, repertoire sequencing, lineage tracing

Posted Date: November 11th, 2022

DOI: https://doi.org/10.21203/rs.3.rs-2231608/v1

Additional Declarations: Yes there is potential Competing Interest. M.S., C.G.R. and H.L.D. are employees of Adimab LLC. and own equity stake in Adimab LLC. L.M.W. is an employee of Invivyd Inc. and owns shares in Invivyd Inc. The other authors declare no competing interests.

Version of Record: A version of this preprint was published at Nature Communications on April 19th, 2023. See the published version at https://doi.org/10.1038/s41467-023-37972-1.

Vaccination of SARS-CoV-2-infected individuals expands a broad range of clonally diverse affinity-matured B cell lineages

Mark Chernyshev[1,*], Mrunal Sakharkar[2,*], Ruth I. Connor[4], Haley L. Dugan[2], Daniel J. Sheward[1], C. Garrett Rappazzo[2], Aron Stålmarck[1], Mattias M.N. Forsell[3], Peter F. Wright[4], Martin Corcoran[1], Ben Murrell[1,#], Laura M. Walker[2,5,#] and Gunilla B. Karlsson Hedestam[1,#]

[1]Department of Microbiology, Tumor and Cell Biology, Karolinska Institutet, Stockholm, Sweden. [2]Adimab LLC, Lebanon, NH 03766, USA. [3]Department of Clinical Microbiology, Umeå University, Umeå, Sweden, [4]Department of Pediatrics, Dartmouth-Hitchcock Medical Center, Lebanon, NH 03756, USA. [5]Invivyd Inc., Waltham, MA 02451, USA

*,# equal contribution

Running title: Boosting polyclonal SARS-CoV-2 antibody responses by vaccination

Keywords: SARS-CoV-2, HCoV, vaccination, monoclonal antibodies, neutralization, repertoire sequencing, lineage tracing

Correspondence:

Gunilla B. Karlsson Hedestam, Department of Microbiology, Tumor and Cell Biology, Karolinska Institutet, S-171 77 Stockholm, Sweden. E-mail: gunilla.karlsson.hedestam@ki.se and Laura Walker, Invivyd, Inc. Waltham, MA 02451, USA. Email: lwalker@invivyd.com

ABSTRACT

Vaccination of SARS-CoV-2 convalescent individuals generates broad and potent antibody responses. Here, we isolated 459 spike-specific monoclonal antibodies (mAbs) from two individuals who were infected with an early ancestral strain of SARS-CoV-2 and later boosted with mRNA-1273. We characterized mAb genetic features by sequence assignments to the donors' personal immunoglobulin genotypes and assessed antibody neutralizing activities against ancestral SARS-CoV-2, Beta, Delta, and Omicron variants. The mAbs used a broad range of immunoglobulin heavy chain (IGH) V genes in the response to all sub-determinants of the spike examined, with similar characteristics observed in both donors. IGH repertoire sequencing and B cell lineage tracing at longitudinal time points revealed extensive evolution of SARS-CoV-2 spike-binding antibodies from acute infection until vaccination five months later. These results demonstrate that highly polyclonal repertoires of affinity-matured memory B cells were efficiently recalled by vaccination, providing a basis for the potent antibody responses observed in convalescent persons following vaccination.

INTRODUCTION

The rapid global spread of SARS-CoV-2 has highlighted the need to understand qualitative aspects of our immune response to emerging and evolving viruses, particularly neutralizing antibody activity and the duration of protective immunity. A wealth of studies has shown that SARS-CoV-2-infected individuals respond with rapid IgG production and neutralizing antibodies that are primarily directed against the receptor-binding domain (RBD) of subdomain 1 (S1) of the virus spike (S). The strength of the early response correlates with disease severity, with persons who experience mild symptoms typically producing lower antibody levels than those who develop moderate or severe disease [1-3]. Serum antibody levels decline gradually once viral replication is controlled and short-lived antibody-producing plasma cells are no longer produced. However, antibody affinity maturation in germinal centers (GCs) continues for several months after the infection. This results in an improved quality of the memory B cell (MBC) compartment, which can be engaged upon re-exposure to antigen [4-6]. Since COVID-19 vaccines became available, many reports have described properties of the elicited immune response; the best studied vaccines being the mRNA vaccines from Moderna [7] and Pfizer/BioNtech [8]. While these vaccines offer high levels of protection against severe disease, the antibody response wanes, and frequent boosting is required to prevent or reduce symptomatic disease [9, 10].

Waning antibody responses and the emergence of multiple SARS-CoV-2 variants of concern (VOCs) that partially or markedly evade antibody responses elicited by previous infection or vaccination have impeded the establishment of durable protection against the virus. Highly transmissible VOCs such as Delta, Omicron, and newly emerging Omicron subvariants reinforce that SARS-CoV-2 is a continuously evolving pathogen. Studies have shown that the individuals who were first infected with SARS-CoV-2 and then vaccinated (sometime referred to as hybrid immunity) develop higher antibody titers and increased neutralization breadth against VOCs compared to those who were only infected or vaccinated [11-16].

While serological studies provide critical information about overall antibody titers and neutralization breadth, qualitative studies of memory B cell (MBC) and plasma cell can greatly help our understanding of how the humoral immune response evolves over time. Here, we applied high-throughput monoclonal antibody (mAb) isolation to retrieve 459 spike-binding mAbs from two individuals who were first SARS-CoV-2 infected and later vaccinated with mRNA-1273 (232 mAbs from donor IML3694 and 227 mAbs from donor IML3695), and we

characterized these for their genetic (germline gene usage, clonality, SHM) and functional (subdomain specificity and neutralization) properties. We then combined this with deep IGH repertoire sequencing (Rep-seq) and mAb linage tracing at longitudinal time points to obtain an improved understanding of the dynamics of the response. Of the 459 spike-binding mAbs, a set of mAbs (n=33) bound both the SARS-CoV-2 and the HCoV-HKU1 spike. The cross-reactive mAbs were found predominantly at the acute infection time point and likely originated from pre-existing MBCs as they displayed significant levels of somatic hypermutation (SHM) already at this time point. In contrast, at the acute infection time point the SARS-CoV-2 S-specific mAbs had low SHM and many of the lineages could be traced to the IgM repertoire, consistent with *de novo* elicitation. Lineage tracing in total IgG repertoires from longitudinal time points demonstrated that the CoV-2 S-specific mAbs diversified and acquired extensive SHM in the five months following the infection, resulting in a highly polyclonal MBC pool that was readily recalled and expanded by the vaccination. These results offer a detailed dissection of the B cell response to SARS-CoV-2 S at a clonal level and over time, illustrating the dynamics of the response in individuals who were infected during the first wave of the pandemic and mRNA vaccinated five months later.

RESULTS

Prior infection results in significantly increased antibody binding and neutralizing titers upon vaccination

We analyzed serum IgG titers against the S proteins of SARS-CoV-2 and HCoV-HKU1 in samples collected from a cohort of individuals who had recovered from the first wave of SARS-CoV-2 infections in 2020, both before and after vaccination, compared to a cohort of uninfected vaccinated individuals and unvaccinated pre-pandemic controls **(Supplementary Table 1)**. Measurable antibody titers against SARS-CoV-2 S were detected in all samples except the pre-pandemic control samples. Responses were highest in individuals who were previously infected then vaccinated, with half-maximal effective concentration (EC_{50}) enzyme-linked immunosorbent assay (ELISA) titers more than an order of magnitude higher than in the same individuals prior to vaccination **(Supplementary Fig. 1A)**. In contrast, antibody titers against HCoV-HKU1 S were similar in the pre-pandemic samples and the samples from uninfected vaccinated individuals, while infected individuals displayed higher HCoV-HKU1 S titers both before and after vaccination **(Supplementary Fig. 1B),** consistent with previous work [6]. Serum samples from donors with prior SARS-CoV-2 infection followed by vaccination displayed higher serum neutralizing titers than samples collected following vaccination alone against all VOCs tested, except the ancestral Wuhan strain (p-value 0.11). Neutralizing antibody titers were significantly higher in serum samples from uninfected vaccinated individuals compared to infected individuals prior to their vaccination **(Supplementary Fig. 1C)**. These data support prior observations that vaccination of SARS-CoV-2 convalescent individuals induces a more robust antibody response than does infection or vaccination alone, and that this response translates into improved serum neutralizing activity against VOCs [11-16].

Isolation and characterization of SARS-CoV-2 spike-specific monoclonal antibodies

To investigate the evolution of the B cell response in more detail, we collected sequential serum and peripheral blood mononuclear cells (PBMCs) from two SARS-CoV-2 recovered individuals, IML3694 and IML3695, who each received a single mRNA-1273 vaccination approximately five months after infection with the ancestral strain. We acquired longitudinal samples from each respective donor as follows: 11 or 14 days post-infection (acute timepoint), 32 or 37 days post-infection (convalescent timepoint), 160 or 169 days post-infection (pre-vax timepoint), and 9 or 7 days post-vaccination (post-vax timepoint) **(Fig. 1A, Supplementary**

Table 2). Assessment of serum neutralizing antibodies showed that the two donors had comparable neutralizing activity against the Wuhan strain (WT), Beta, Delta, and Omicron BA.1. Beta and Omicron BA.1 were more neutralization-resistant than the WT, and the Delta variants **(Fig. 1B)**, as previously reported [17-22]. A total of 459 spike-specific mAbs were isolated across the acute, pre-vax, and post-vax time points, 232 from IML3694 and 227 from IML3695 **(Supplementary Table 3).** The mAbs were isolated from total antibody-secreting cells (ASCs) at the acute and post-vax time points and from spike-binding MBCs at the pre-vax time point (**Supplementary Fig. 2A**). The subdomain specificities of the mAbs were determined by binding to recombinant SARS-CoV-2 subdomain 2 (S2), N-terminal domain (NTD) and receptor binding domain (RBD) proteins. S2-specific antibodies dominated the response in both donors **(Fig. 1C)**, consistent with previous observations [6, 23]. When examining mAbs isolated at the three different time points separately, we observed differences in IGHV gene usage with a proportionally lower use of IGHV1 and IGHV4 family genes at the acute infection time compared to the other time points. This was largely explained by the fact that proportionally more HCoV-HKU1-binding mAbs were isolated from this time point (**Supplementary Fig. 2B**), many of which used IGHV3-30 (IGHV3-30*18). We also observed a peak of IGHV1-69-using mAbs post-vaccination, which included several (n=21) clonally diverse IGHV1-69-using antibody lineages that were readily expanded by vaccination (**Supplementary Fig. 3A**). This skewing between mAbs isolated at different time points was also apparent at the level of subdomain specificities. mAbs isolated from the acute infection time point showed a different distribution of subdomain specificities compared to those isolated from pre- and post-vax time points due to the frequency of HCoV-HKU1 cross-reactive lineages at the acute time point. Despite binding to the full-length trimeric SARS-CoV-2 S, many of these could not be mapped to a specific subdomain, possibly due to low affinity or the lack of quaternary epitopes on the probes used here (**Supplementary Fig. 3B)**. The subdomain specificities of mAbs isolated at different time points were very similar between the two donors and consisted of S2, NTD and RBD binders (**Supplementary Fig. 3C**).

We next assigned germline immunoglobulin heavy chain V, D and J (IGHV, IGHD and IGHJ) allele usage to each mAb. To ensure correct assignment, personalized IG genotyping was performed using IgDiscover [24] to infer germline IG alleles from expressed IgM repertoires from each donor (**Supplementary Table 4**). Correct allelic assignment is required not only for correct clonotyping of antibodies but also for precise calculations of SHM. The SARS-CoV-2

S-specific mAbs used a broad range of IGHV genes, with IGHV3-9, IGHV3-30, IGHV3-30-3, IGHV3-33, IGHV4-31, IGHV1-69, and IGHV4-59 being the most frequently used. We found that the gene usage was highly similar between the two donors, demonstrating inter-donor consistency in the engagement of the B cell repertoire against SARS-CoV-2 **(Fig. 1D).** Most of the IGHV genes were used in the response to all three subdomains, RBD, NTD and S2, except IGHV3-53 and IGHV2-5, which were almost exclusively used in the Ab response to RBD **(Fig. 1E)**. Biased IGHV gene usage in the RBD response is consistent with previous work [25-29].

Of the full panel of mAbs described in this study, 31 displayed neutralizing half-maximal inhibitory concentration (IC_{50}) values below 0.4 mg/ml against SARS-CoV-2, and four mAbs (ADI-67444, ADI-67138, ADI-67183 and ADI-67857) potently neutralized Omicron BA.1 with IC_{50} values below 0.02 mg/ml **(Fig. 2)**. Since all mAbs were isolated prior to the emergence of the Omicron lineage and prior to the use of Omicron variant vaccines, these results demonstrate the ability of the immune system to generate antibodies against epitopes that are conserved between the ancestral spike and VOCs, despite numerous mutations in the RBD of many variants. Of the four Omicron BA.1 neutralizing mAbs, three potently neutralized the Omicron sub-lineage, BA.2.75, yet all failed to neutralize the Omicron sub-lineage BA.5 **(Fig. 2)**.

Bulk antibody repertoire sequencing for lineage tracing

To examine the evolution of the B cell lineages defined by the isolated mAbs, we produced bulk IgG libraries from each donor using PBMCs sampled at the acute infection, convalescent and post-vax time points. To analyze B cell repertoire diversity rather than transcript counts, the Rep-seq VDJ nucleotide sequences were deduplicated and denoised using the Fast Amplicon Denoising (FAD) algorithm [30]. An example of a traced antibody lineage before and after FAD is shown in **Supplementary Fig. 4A**. We also observed that some of the high SHM sequences were the result of apparent chimeric products, likely formed during PCR, which we filtered out using a chimeric IGHV sequence detection method. The effect of chimeric cleaning was visible when examining individual antibody lineages with chimeric sequence average SHM consistently falling above the average SHM for the non-chimeric sequences **(Supplementary Fig. 4B)**. All subsequent tracing analysis was performed following FAD and chimera cleaning. The ratio of clonotypes to unique sequences was higher on average (0.86 with standard deviation of 0.03) for IgM compared to IgG repertoires (0.27 with standard

deviation of 0.05), which may be explained by IgG repertoires being more heavily dominated by expanded clones **(Supplementary Fig. 4C)**. We observed that IGHV3-30 and IGHV3-33 usage was high across all repertoires, especially for IgG **(Supplementary Fig. 4D)**. IGHV3-23 was among the most frequently used genes in the IgM repertoires, especially in IML3695, but it was not often used proportionally in the S-specific mAbs.

Lineage analysis reveals the development of spike-binding antibodies following infection and vaccination

Of the HCoV-HKU1 cross-reactive mAbs isolated from the different time points, 48% were isolated from the acute infection time point (**Fig. 3A**). When comparing SHM levels for the HCoV-HKU1 cross-reactive mAbs (n=16) with SARS-CoV-2 spike-specific mAbs (n=50) from the acute infection time point, we observed a significant difference in median SHM levels: 7.56% compared to 3.49% respectively at the nucleotide level (**Fig. 3B**). This suggested that pre-existing HCoV-HKU1 memory B cells were reactivated by SARS-CoV-2 infection in these donors, consistent with the serological data (**Supplementary Fig. 1**) and previous reports [31]. To investigate this further, we selected an HCoV-HKU1 spike cross-reactive lineage, ADI-66175, for tracing in the IgG Rep-seq data. The ADI-66175 lineage was represented by 7 clonally related mAbs from the complete mAb set (**Supplementary Table 3**).

Tracing an expanded HCoV-HKU1 S-cross-reactive lineage, ADI-66175, in the IgG Rep-seq data revealed that it evolved extensively during the acute SARS-CoV-2 infection. This lineage was especially rich with numerous somatic variants traced at the acute infection time point and a smaller number at the convalescent time point (**Fig. 3C**). The full range of SHM detected for this lineage suggested that a range of variants, from unmutated to intermediate to highly mutated, were archived in memory B cells. We did not identify any members of this lineage in the IgM libraries, supporting the conclusion that this was a pre-existing IgG-switched lineage.

We next evaluated three SARS-CoV-2 S-specific lineages for which large numbers of somatic variants were traced, ADI-66196 and ADI-67860, S2-specific Abs, and ADI-67983, an RBD-specific neutralizing Ab. ADI-66196 was isolated at the acute infection time point and had very low SHM, while ADI-67860 and ADI-67983 were isolated from the pre-vax time point and had higher SHM. Variants of the three mAbs were traced in both IgM and IgG libraries from the acute infection time point when both ASCs and MBCs are likely to be present, while almost no sequences could be traced at the convalescent time point, suggesting that the memory B cell pool was small or contracted. However, extensive expansion was observed for both lineages at

the post-vax time point with multiple distinct evolutionary branches as demonstrated by phylogenetic tree analysis (**Fig. 4A**). SHM comparisons between the mAbs and the traced sequences illustrated the increase in SHM between the acute infection time point and the post-vax time point (**Fig. 4B**). Because the post-vax time point was as early as 7 or 9 days after vaccination, the high SHM levels observed at this time likely reflected affinity maturation that had occurred in the time leading up to the vaccination, archived in memory B cells, rather than an increase in SHM following vaccination. The fact that ADI-67983, which was isolated at the pre-vax time point, had similar SHM levels as its traced somatic variants at the post-vax time point illustrates this point. Furthermore, these analyses highlight that inclusion of IgM in lineage tracing bridged the gap between disparate clades of IgG sequences, aiding the construction of lineage trees.

Vaccination expands a broad range of infection-induced S-specific Ab lineages

Having confirmed that SARS-CoV-2-specific B cell lineages could be traced in bulk Rep-seq data from the post-vax time points for selected mAb sequences, we performed a broader search that included all infection-induced SARS-CoV-2 S-specific Ab lineages, defined either by mAbs that were isolated pre-vax, or by mAbs that were isolated from the post-vax time point but which could be traced back to a time point prior to the vaccination. Clonal collapsing revealed that the 459 mAbs belonged to 405 mAb lineages of which 200 (49.4%) were traceable in the next-generation sequencing (NGS) data at one or several time points, including 13 neutralizing lineages. Traced lineages were assigned to the subdomain specificities of the corresponding mAbs, which resulted in a total of 82 S2 lineages, 33 NTD lineages, 32 RBD lineages, and 53 lineages with undefined subdomain specificity. The subdomain specificity proportions among lineages were consistent with the proportions among the mAbs, with S2 lineages being the most common and NTD and RBD present at similar numbers.

Strikingly, analysis of the IgG libraries generated from day 9 (IML3694) and day 7 (IML3695) after vaccination demonstrated that vaccination expanded a broad range of B cell lineages, with 88 clonally distinct lineages in the two donors. This included lineages defined by mAbs isolated from MBCs at the pre-vax time point (n=52) and lineages defined by mAbs that were isolated at other time points and traced both before and after the vaccination (n=36). Overall, these results suggest that the vaccine-induced recall response engaged a highly polyclonal B cell repertoire, including several neutralizing Ab lineages **(Fig. 5A)**. For most lineages, we observed

a decrease in traceable sequences during the convalescent timepoint compared to the acute timepoint, which may be explained by either a contraction in SARS-CoV-2 spike-specific MBCs or a lack of circulating S-specific ASCs at this time point. Interestingly, we identified a set of S-specific lineages (ADI-66210, ADI-66213, ADI-66196, ADI-66197, ADI-67108, ADI-67109 and ADI-67112) that were present both at the acute infection time point, when these mAbs were isolated from ASCs, and as MBCs that could be reactivated by the vaccination five months later, suggesting dual differentiation fates for infection-induced B cells.

When we examined the median level of SHM in lineages that were traced in both IgM Rep-seq data from the acute infection time point and IgG Rep-seq data from the post-vax time point there was a clear increase in SHM in all lineages (**Fig. 5B, left**). A similar effect was observed in lineages traced in IgG Rep-seq data from the acute infection time point and IgG Rep-seq data from the post-vax time point (**Fig. 5B, right**). We also compared SHM levels of the mAbs that were isolated from MBCs at the pre-vax time point with the median SHM of their variants that were traced at the post-vax time point. We found the SHM levels to be highly similar, consistent with affinity maturation having occurred during the time leading up to the vaccination rather than in the short period (9 or 7 days) between the vaccination and the post-vax sampling time point (**Fig. 5C**). Thus, the peak in serum antibody titers observed one week after vaccine boosting (**Fig. 1B**) reflects antibody sequences archived in MBCs and their differentiation into antibody-secreting plasmablasts upon antigen restimulation.

DISCUSSION

The SARS-CoV-2 pandemic is unique due to its rapid spread and extensive impact on societies, and because vaccines were developed and deployed within just a year of isolating the virus. Vaccination has curtailed the damage caused by the pandemic by protecting individuals from severe disease. Two mRNA-based vaccines, mRNA-1273 from Moderna and BNT162b2 from Pfizer/BioNTech, were among the first COVID-19 vaccines to be approved, with several inactivated virus- and vector-based vaccines gaining approval around the same time or soon thereafter. At present, several billion doses of mRNA vaccines have been administered globally, with numbers increasing rapidly. However, availability of the vaccines was initially limited and, while this has improved, access to vaccine doses remains constrained in many parts of the world. Thus, with the continued spread of the virus, the first exposure to SARS-CoV-2 for many persons is natural infection, making studies of how convalescent persons respond to subsequent vaccination highly relevant. Several studies have shown that immunity induced by infection followed by vaccination stimulates higher antibody titers than either alone [11, 14, 15], but how the B cell response evolves following infection and vaccination remains a question of interest.

To investigate this question, we used a high throughput mAb isolation platform to generate 459 spike-specific mAbs representing 405 clonally unique Ab lineages from two individuals who were first infected with SARS-CoV-2 and vaccinated with a single dose of mRNA-1273 about five months later. Characterization of the mAbs at the genetic and binding levels revealed that they used a broad set of IGHV genes to target all subdomains of the spike analyzed (RBD, NTD and S2), illustrating the polyclonal nature of the response. We identified 31 mAbs that neutralized one or more SARS-CoV-2 variants, including four mAbs that potently neutralized the recently emerged Omicron BA.2.75 variant. Neutralization of BA.5, which was responsible for the fifth wave of infections in South Africa [32] and then rapidly spread to become dominant in many parts of the world, was weak, if detectable. Escape from neutralizing antibodies by BA.5 is well-documented [33, 34] and our results are consistent with recent findings showing that BA.2.75 is, for some antibodies, more neutralization-sensitive than BA.5 [21].

A set of non-neutralizing mAbs (n=33) were cross-reactive with the spike of HCoV-HKU1, the majority of which were isolated at the acute infection time point when total ASCs were used as the source for mAb isolation. Consistent with prior studies, the cross-reactive mAbs displayed overall higher levels of SHM than the SARS-CoV-2 spike-specific mAbs isolated at the same time point, suggesting that SARS-CoV-2 infection boosted pre-existing cross-reactive MBCs induced by prior infection with endemic HCoVs, such as HKU1 [6, 31, 35]. The HCoV-HKU1

cross-reactive Ab lineage that we studied in-depth, ADI-66175, evolved additional SHM through the convalescent phase, but it was not boosted by vaccination suggesting that it recognized an epitope that was not present on the vaccine antigen. Whether HCoV cross-reactive antibody responses have a protective role and contribute to the control of SARS-CoV-2 remains unknown. Other studies have shown that HCoV cross-reactive Abs are mostly S2-directed, and such Abs are, with rare exceptions [36], non-neutralizing. In our study, we could not define the domain specificity for all 33 HCoV-HKU1-binding mAbs but we could show that they were non-neutralizing. This does not rule out that they play a role in antibody-dependent cellular cytotoxicity (ADCC) or other antibody-dependent immune functions that were not studied here.

The greatest benefit of this collection of mAbs was the opportunity to use their sequences to interrogate the B cell repertoire longitudinally. A primary objective of the study was to determine if there were constraints in the recall response that skewed or limited the post-vaccination response to a more oligoclonal repertoire. Boosting a broad repertoire of B cells is desired as this provides improved chances to maintain effective neutralizing antibody responses in the face of viral evolution and the emergence of VOCs. To address this question, we deep-sequenced IgG repertoires from the acute infection time point, as well as from the pre- and post-vax time points. The post-vax time point approximately one week after vaccination was selected to capture the burst of short-lived ASCs that originate from pre-existing MBCs [37, 38]. The fact that we could trace as many as 88 SARS-CoV-2 S-specific infection-induced antibody lineages at the post-vax time point demonstrates that mRNA-1273 vaccination of previously SARS-CoV-2-infected individuals stimulates a very broad repertoire of MBCs generated from the infection. In both donors, this included RBD-targeting neutralizing Ab lineages, ADI-67649, ADI-67748 and ADI-67831 in IML3694 and ADI-67135, ADI-67857, ADI-67971 and ADI-67983 in IML3695. Additional but less expanded RBD-neutralizing lineages were also observed post-vaccination. The lineage tracing allowed us to identify many clonal variants of each antibody lineage and construction of phylogenetic trees illustrated the high degree of diversification and maturation that each lineage undergoes during the months following SARS-CoV-2 infection. Similar studies have been performed in influenza-vaccinated subjects, also demonstrating continued evolution of pre-existing influenza-specific B cell lineages following vaccination [39].

While it is not expected that all lineages that are present in a donor can be traced from a single blood draw due to sampling limitations, we conclude that many lineages archived in the MBC

pool could be measured at the post-vax time point when they likely contributed to the increase serum antibody titers. Several mAbs isolated from MBCs sampled at the pre-vax time point that were traced at the post-vax time point, which was 9 and 7 days later for IML-3694 and IML-3695 respectively, had similar SHM levels between these two time points. These results are consistent with that sequences traced at the post-vax time point originate from reactivated MBCs that differentiate into plasmablasts 7 to 9 days after the vaccination without having undergone further affinity maturation in the GC (**Figure 5C**). Whether infection-induced spike-specific IgG-switched MBCs are recruited back to GCs upon vaccine boosting was not investigated here due to the lack of later sampling time points for these donors. While it has been shown that increases in SHM within given B cell lineages result from persistent GCs over long periods of time [40], the extent to which circulating MBCs are recruited back into GCs in response to antigen boosting remains a topic of intense research [41]. Furthermore, in addition to the circulating blood compartment sampled here, MBCs also reside in tissues [42, 43]. As such compartments were not sampled here, this study likely underestimates the diversity of SARS-CoV-2 S-specific Ab sequences that were recalled by the vaccination.

Overall, our approach involving mAb isolation coupled with lineage tracing in bulk IgG libraries allowed us to comprehensively probe the SARS-CoV-2 S-specific MBC repertoire. The results underscore the polyclonal nature of the infection-induced Ab response and show that vaccination of convalescent persons expands a broad repertoire of Ab lineages, underpinning the effective responses observed in hybrid immunity.

METHODS

Study design and donor information

The results shown in Supplementary Fig. 1A were performed under permit 2021-00055 and amendment 2021-01387 approved by the Swedish ethics review authority and is part of an ongoing clinical trial to investigate immune responses to Covid-19 vaccination (EudraCT number 2021-000683-30). Two SARS-CoV-2-infected patients were recruited for in-depth studies. Both volunteers gave informed consent in accordance with the Dartmouth-Hitchcock Hospital (D-HH) Human Research Protection Program (Institutional Review Board) and approved by the Swedish ethics review authority, permit 2021-01850. SARS-CoV-2 infection was confirmed by reverse transcriptase polymerase chain reaction after nasal swab in October 2020. Participants received the first dose of the mRNA-1273 vaccine (Moderna) approximately 5 months after the first positive test. Blood samples were collected and fractionated by the Clinical Research Unit of D-HH to obtain PBMCs and serum. Donor information and sample collection dates are shown in **Supplementary Table 2**.

Recombinant antigens

Prefusion-stabilized SARS-CoV-2 spike protein (S-2P) was generated using a plasmid encoding residues 1-1208 of the SARS-CoV-2 spike. Other features of the plasmid include a mutated S1/S2 furin cleavage site (RSAR to GSAS), proline substitutions at positions 986 and 987, a C-terminal T4 fibritin domain, HRV3C cleavage site, 8x HisTag and TwinStrepTag. HEK-293 cells (DSMZ, ACC 305) were transfected using PEIpro (PolyPlus, Cat# 115-100), followed by addition of Kifunensine (5 μM) after 3-hr. Cell supernatants were harvested and expressed protein was purified using NiNTD Sepharose resin (Cytiva, Cat# 17531804) and StrepTactin XT Superflow high-capacity resin (IBA Life Sciences, Cat# 24030025). Using size exclusion chromatography, purified protein was polished successively on a HiLoad 16/600 Superdex 200 pg column (Cytiva, Cat#28989335) and HiLoad 16/600 column packed with 125 mL of Superose 6 resin (Cytiva, Cat# 17048901). Plasmids encoding residues 319-591 of the SARS-CoV-2 spike with a C-terminal HRV3C cleavage site, monomeric Fc-tag and 8x HisTag (SARS-CoV-2 RBD-SD1); residues 1-305 of the SARS-CoV-2 spike with a C-terminal HRV3C cleavage site, monomeric Fc-tag and 8x HisTag (SARS-CoV-2 NTD) were transfected into FreeStyle293F cells using polyethylenimine. Cell supernatants were harvested after 6 days and purified using Protein A resin (Pierce). Affinity-purified SARS-CoV-2 RBD-SD1 and NTD

proteins were then further polished by size-exclusion chromatography on a Superdex 200 Increase column (Cytiva) in a buffer composed of 2 mM Tris pH 8.0, 200 mM NaCl and 0.02% NaN3. The SARS-CoV-2 spike S2 protein was purchased from Acro Biosystems (Cat# S2N-C52H5) and HCoV-HKU1 S (Cat# 40606-V08B) protein was purchased from Sino Biological.

Detection and sorting of single B cells

Acute samples post-infection and samples post-vaccination were stained to isolate antibody secreting cells (ASCs), whereas pre-vaccination PBMCs were stained for memory B cells (MBCs). For ASC sorts, PBMCs were stained using anti-human CD19 (PE-Cy7; Biolegend, Cat# 302216), CD20 (APC-Cy7; Biolegend, Cat302313#),CD38 (PE; Biolegend, Cat# 303506), CD3 (PerCP-Cy5.5; Biolegend, Cat# 30040), CD8 (PerCP-Cy5.5; Biolegend, Cat# 344710), CD14 (PerCP-Cy5.5; Invitrogen, Cat# 45-0149-42), CD16 (PerCP-Cy5.5; Biolegend, Cat# 360712), IgM (BV711; BD Biosciences, Cat# 747877), CD71 (APC; Biolegend, Cat# 334107), CD27 (BV510; BD Biosciences Cat# 740167) and propidium iodide (PI). For MBC sorts, PBMCs were stained with CD19 (PE-Cy7; Biolegend, Cat# 302216), CD3 (PerCP-Cy5.5; Biolegend, Cat# 30040), CD8 (PerCP-Cy5.5; Biolegend, Cat# 344710), CD14 (PerCP-Cy5.5; Invitrogen, Cat# 45-0149-42), CD16 (PerCP-Cy5.5; Biolegend, Cat# 360712), IgM (BV711; BD Biosciences, Cat# 747877), CD71 (APC-Cy7; Biolegend, Cat# 334110), CD27 (BV510; BD Biosciences, Cat# 740167), PI and a freshly-prepared mixture of PE- and APC-labeled SARS-CoV-2 S-2P protein tetramers (25 nM each). ASCs, defined as $CD19^{+}CD20^{lo}CD38^{+}CD27^{+}CD3^{-}CD8^{-}CD14^{-}CD16^{-}PI^{-}$ or class-switched B cells, defined as $CD19^{+}CD3^{-}CD8^{-}CD14^{-}CD16^{-}PI^{-}IgM^{-}IgD^{-}$ cells that showed reactivity to both SARS-CoV-2 S-2P tetramers, were single-cell index sorted using a BD FACS Aria II Fusion (BD Biosciences) into 96-well polypropylene microplates (Corning Cat# 07-200-95) containing 20 µl/well of lysis buffer [5 µl of 5X first strand SSIV cDNA buffer (Invitrogen Cat # 18090050B), 0.25 µl RNaseOUT (Invitrogen Cat#10777019), 0.625 µl of NP-40 (Thermo Scientific Cat# 85124),1.25 µl dithiothreitol (Invitrogen), and 12.85 µl dH_2O]. Plates were spun down at 1,000 × g for 30 s and stored at -80°C until use. Flow cytometry data was analyzed using FlowJo software.

Amplification and cloning of antibody variable genes

Human antibody variable gene transcripts (VH, Vκ, Vλ) were amplified by reverse transcription polymerase chain reaction (RT-PCR) using SuperScript IV enzyme (Thermo Scientific Cat# 18090050) followed by nested PCR using HotStarTaq Plus DNA Polymerase (Qiagen Cat#

203646) and a mixture of IgM-, IgD-, IgA- and IgG-specific constant-region primers as previously described (Wec et al. Science 2020). The primers used in the second round of nested PCR contained 40 base pairs of 5′ and 3′ homology with linearized yeast expression vectors to allow cloning by homologous recombination. Amplified transcripts were transformed into *S. cerevisiae* using the lithium acetate method for chemical transformation [44]. Per transformation reaction, yeast cells ($1x10^7$) were incubated with a mixture of 240 µl of polyethylene glycol (PEG) 3350 (50% w/v) (Sigma-Aldrich, Cat# 202444), 36 µl of 1M lithium acetate (Sigma Aldrich, Cat# 517992), 10 µl of denatured salmon sperm DNA (Invitrogen, Cat# 15632011), 67 µl sterile water, 200 ng of each of the digested vectors and 10 µl each of unpurified VH and VL amplified PCR product at 42°C for 45 min. Yeast were then washed twice with sterile water, recovered in selective media, and plated for Sanger sequencing.

Expression and purification of IgGs and Fab fragments

To produce monoclonal antibodies (mAbs) as full-length IgG1 proteins, *S. cerevisiae* yeast cultures were incubated in 24 well plates at 30°C and 80% relative humidity with shaking at 650 RPM in Infors Multitron shakers. Culture supernatants were harvested after 6 days and IgGs were purified by protein A-based affinity chromatography followed by elution using 200 mM acetic acid with 50 mM NaCl (pH 3.5) and finally neutralized with 1/8 (v/v) 2 M HEPES (pH 8.0). To generate Fab fragments, IgGs were digested with papain at 30°C for 2-hr and the reaction terminated using iodoacetamide. To remove Fc fragments and undigested IgG, the mixtures were passed over protein A agarose. The flow-through was then passed over CaptureSelect™ IgG-CH1 affinity resin (ThermoFisher Scientific) and the Fabs captured on the resin surface were eluted using 200 mM acetic acid with 50 mM NaCl (pH 3.5) followed by neutralized 1/8 (v/v) 2 M HEPES (pH 8.0).

Biolayer interferometry kinetic measurements

Apparent equilibrium dissociation constant (K_D^{App}) affinities were calculated by BLI using a ForteBio Octet HTX instrument (Molecular Devices) as previously described [45]. Reagents were formulated in PBSF (PBS with 0.1% w/v BSA), and all binding steps were performed at 25°C with 1000 rpm orbital shaking speed. To measure IgG binding to recombinant antigens, IgGs (100nM) were captured on anti-human IgG (AHC) biosensors (Molecular Devices) and then equilibrated in PBSF for a minimum of 30 min. Following a 60-s baseline step in PBSF, the IgG-loaded biosensors were exposed to the antigen at 100 nM for 180-s and then dipped into PBSF to measure any dissociation of the antigen from the biosensor surface over a period

of 180-s. For binding responses > 0.1 nm, data were aligned, inter-step corrected (to the association step), and fit to a 1:1 binding model using the ForteBio Data Analysis Software, version 11.1.

SARS-CoV-2 spike-pseudotyped MLV neutralization assay

Single-cycle infection pseudoviruses were generated as previously described [46]. Briefly, HEK-293 cells were co-transfected with 0.5 µg of the SARS-CoV-2 WT spike (NC_045512; pCDNA3.3) or SARS-CoV-2 variants (Beta, Delta, Omicron BA.1) and 2 µg each of MLV luciferase (Vector Builder) and MLV gag/pol (Vector Builder) plasmids using Lipofectamine 2000 (ThermoFisher Scientific). Cell supernatants were harvested 48-hr post-transfection and aliquoted to be frozen at -80°C. To measure neutralizing activity of mAbs, 10,000-15,000 HeLa-hACE2 cells/well (BPS Bioscience Cat #79958) were seeded overnight in 96-well tissue culture plates (Corning). Serial dilutions of mAbs (4 mg/ml-0.5 ng/ml) in cell culture media were incubated with a fixed volume of MLV particles for 1-hr at 37°C, 5% CO_2. After washing HeLa-hACE2 cells three times with DPBS, the virus-mAb mixture was directly added over the cells and incubated. After 72-hr, the supernatant was aspirated and cells were lysed with Luciferase Cell Culture Lysis 5× reagent (Promega, Cat# E153A). Luciferase activity was measured using the Luciferase Assay System (Promega, Cat# E151A) following manufacturer's instructions, and relative luminescence units (RLU) were quantified on a luminometer (Perkin Elmer). Percent neutralization was calculated as $100*(1–RLU_{sample}/RLU_{isotype\ control\ mAb})$, and the 50% neutralization concentration was interpolated using four-parameter nonlinear regression fitted curves in GraphPad Prism.

VSV-SARS-CoV-2 pseudovirus neutralization assay

Microneutralization assays were also performed using a VSV-based pseudovirus system as previously described (Butler et al. Frontiers in Imm 2020). Briefly, mAbs or serum were diluted in 2-fold series and incubated with VSV-SARS-CoV-2 pseudoviruses for 1 hr at 37°C. The mixture was then added to 293T-hsACE2 cells (Integral Molecular, Philadelphia, PA) and incubated at 37°C, 5% CO_2 for 24 hrs. Cell lysates were collected and luciferase activity measured using the Bright-Glo system (Promega) with a Bio-Tek II plate reader. Percent neutralization was calculated as [100 - (mean RLU test wells/mean RLU positive control wells) × 100] and further used to determine the half-maximal inhibitory concentrations for mAbs (IC_{50}) and 50% neutralization titers for serum (NT_{50}).

Enzyme-linked immunosorbent assays (ELISA)

For serum binding studies, SARS-CoV-2 S-2P protein was diluted to 5 µg/ml in PBS (pH 7.4) and used to coat 96-well high-binding polystyrene ELISA plates (Corning, Cat# 3690) were coated with 25 µl per well of SARS-CoV-2 S-2P protein diluted to 5 µg/ml in PBS (pH 7.4) and incubated overnight at 4°C. All subsequent incubations, until the addition of substrate, were for 1-hr at 37°C. Wells were washed 3 times with PBS and incubated with blocking solution (5% (w/v) non-fat dried milk (NFDM)). Serial dilutions of human serum were prepared in 5% NFDM-PBS and added to the wells (25 µl per well) after removal of the blocking solution. Plates were washed three times with PBS followed by addition of secondary cross-adsorbed anti-human IgG-HRP (Thermo Fisher Scientific, Cat# 31413) detection antibody (25 µl per well) at 1:8000 dilution in 5% NFDM-PBS. Plates were washed three times with PBS. 1-Step Ultra TMB-ELISA Substrate Solution (Thermo Fisher Scientific, Cat# 34029) was added (25 µl per well) to detect binding, incubated at room temperature for 6-8-min followed by addition of an equal volume of stop reagent (2M sulfuric acid). Absorbance was measured at 450 nm using a Spectramax microplate Reader (Molecular Devices) and responses plotted as a function of dilution. Serum binding was calculated as the area under the curve using GraphPad Prism (version 9).

Repertoire sequencing analysis

IgDiscover [24] v0.15.2 was used to preprocess IgM/IgG libraries, annotate VDJ sequences, and infer individualized V, D, and J germline genotypes for the donors from the IgM libraries using the IMGT release 202141-1 (11 October 2021) as a starting database. IgBLAST annotated NGS VDJ sequences were denoised and deduplicated using Fast Amplicon Denoising (FAD) with an error rate of .0047, which is the median MiSeq error rate reported by Illumina [47]. We applied FAD [30] to reduce the prevalence of singleton sequences that differ by only one nucleotide as these are more likely to represent different RNA templates from the same cell. This approach increases the likelihood that the traced sequences represent unique cells. Chimeric sequences were detected using a hidden Markov model (HMM) based approach. Briefly, the method generates an HMM based on an individual's personalized IGHV genotype. The V region of each query sequence is modeled as either being derived from a single IGHV allele with mutation or allowing template switching between different IGHV alleles (also with mutation, with mutation rates potentially differing between the different component templates). Comparing the two models' likelihoods provided us with a Bayes factor; we set a log10 Bayes factor of >5 as our threshold for chimera detection.

Lineage tracing

Lineage tracing was performed on combined IgM Rep-seq, IgG Rep-seq, and mAb data with the IgDiscover clonotypes command [48]. A clonotype was defined as all sequences with the same V and J allele assignment, identical HCDR3 nucleotide lengths, and in the same single linkage cluster with a cutoff of 0.8 nucleotide match fraction between HCDR3 nucleotide sequences. Lineages with multiple mAbs which had differing light chain assignments were sub split by first creating new clones for each light chain VJ combination, then reassigning the heavy chain Rep-seq sequences from the original clone to the sub split lineage containing the mAb heavy chain sequence with the smallest possible Levenshtein distance. Clonotypes consisting of Rep-seq sequences and mAb sequences were given subdomain specificities and HCoV-HKU1 S binding data based on the mAbs they contain. If any of the mAbs in a clone had different subdomain specificities or an undefined subdomain specificity, the clone was marked as having an undefined subdomain specificity.

EC_{50} calculation

Serum EC_{50}s were generated by fitting a logistic curve against the $\log_{10}$ of the dilution factors using the nlsLM function from the minpack.lm R package. The logistic curve's maximum value was set to be the same across each antigen, with 1.364444 for anti-SARS2 S IgG and 1.818325 or anti-HCoV-HKU1 S IgG. These maximum values were computed as the median of per donor maximums across all readings for each antigen. Anti-SARS2 S IgG maximums below .5 were excluded from the median calculation because they were low outliers from the pre-pandemic timepoint. Signals that were too low and flat to fit a logistic curve were given an EC_{50} equal to 100, which is the smallest dilution factor.

Phylogenetic tree construction

All phylogenetic trees were created by first aligning nucleotide sequences using MAFFT v7.490 [49], then generating maximum-likelihood trees using FastTree double precision v2.1.11 [50]. Visualization was performed using ggtree v3.2.1 [51].

Code availability

IgDiscover22 v1.0.0 is available at https://gitlab.com/gkhlab/igdiscover22, scripts used to generate all results in the paper are available at https://gitlab.com/gkhlab/Vaccination_of_SARS-CoV-2_Convalescents, and HMM code for chimera identification is available at https://github.com/MurrellGroup/CHMMera/

FIGURE LEGENDS

FIG. 1 | Study design, serum neutralizing activity and properties of spike-binding monoclonal antibodies (mAbs). **(A)** Schematic of study design with time points for infection and vaccination, mAb isolation, and samples for NGS. **(B)** IML3694 and IML3695's serum neutralizing antibody values against ancestral SARS-CoV-2 Wuhan (WT) and variants of concern (VOCs). **(C)** Pie chart of mAb subdomain specificities in the two donors. **(D)** mAb IGHV allele frequencies colored by donor. **(E)** mAb IGHV allele frequencies colored by subdomain specificity.

FIG. 2 | A summary of all neutralizing mAbs with an IC_{50} below 0.4 mg/ml against any of the SARS-CoV-2 VOCs.

FIG. 3 | Isolation time point and evolution of HCoV-HKU1 S cross-reactive mAbs. **(A)** Pie chart of timepoints in which HCoV-HKU1 S-binding mAbs were isolated. **(B)** Dot plot of % nucleotide IGHV SHM for the HCoV-HKU1 S cross-reactive and SARS-CoV-2 S-specific mAbs isolated at the acute timepoint. Mann-Whitney U test used for comparison. **(C)** Maximum likelihood phylogenetic trees of HCoV-HKU1 S-binding traced lineage ADI-66175. The germline sequence was obtained from the IgBLAST generated "germline_alignment" column of the sequence with the minimum IGHV SHM in the lineage.

FIG. 4 | Evolution of SARS-CoV-2 S-specific antibody lineages over the sampling time points. **(A)** Maximum likelihood phylogenetic trees of traced lineages containing IgM Rep-seq sequences: ADI-66196, ADI-67860, and ADI-67983. Germlines sequences were obtained from the IgBLAST generated "germline_alignment" column of the sequence with the smallest IGHV SHM in the lineage. **(B)** Dot plot of % nucleotide IGHV SHM for the ADI-66196, ADI-67860, and ADI-67983 lineage sequences. Purple crossbars represent mAb values, while the blue crossbars represent average values of traced variants for each timepoint.

FIG. 5 | IgM and IgG repertoire sequencing and lineage tracing of SARS-CoV-2 S-specific antibody lineages at the longitudinal time points. **(A)** Bubble plots of SARS-CoV-2 S-specific mAb lineages found before and after vaccination in IML3694 and IML3695. The bubble sizes correspond to post-FAD and chimera cleaned data. **(B)** Line plots of median % nucleotide IGHV SHM for lineages found in acute IgM/IgG and post-vax IgG Rep-seq data. **(C)** Boxplot of median % nucleotide IGHV SHM for lineages containing pre-vax timepoint mAbs and post-vax IgG Rep-seq. Wilcoxon signed-rank test used for comparison.

Supplementary data

Supplementary Fig. 1 | Serum IgG titers against the SARS-CoV-2 **(A)** and HCoV-HKU1 S glycoproteins **(B)** as well as neutralizing antibody titers against SARS-CoV-2 WT and variants **(C)** in a cohort of individuals a median of 8 days (range: 7-14) days after vaccination by mRNA-1273 (n = 22) or BNT162b2 (n = 21), 22 of whom were previously infected with SARS-CoV-2 (Recovered) and given one dose and 21 who were not previously infected (Unexposed) and given two doses. The previously infected individuals were vaccinated a median of 179 days after disease onset (range: 40-213 days). For these individuals, we also included serum samples collected a median of 42 (range 0-176 days) days before the mRNA vaccination. We used Mann-Whitney U-tests to compare titers. *P < 0.05, **P < 0.01, ***P < 0.001, and ****P < 0.0001.

Supplementary Fig. 2 | (A) Flow cytometry plots showing the staining and gating strategy for sorting ASCs and spike-specific MBCs. **(B)** Number of HCoV-HKU1 and SARS-CoV-2 S cross-reactive mAbs versus SARS-CoV-2 S-specific mAbs isolated at the different time points.

Supplementary Fig. 3 | (A) mAb IGHV allele frequencies colored by donor shown separately for the three sets of mAbs isolated at the different time points. **(B)** mAb IGHV allele frequencies colored by subdomain specificity shown separately for the three sets of mAbs isolated at the different time points. **(C)** Pie charts of mAb subdomain frequencies shown separately for the three sets of mAbs isolated at the different time points.

Supplementary Fig. 4 | (A) Maximum likelihood phylogenetic tree of IgM NGS, IgG NGS, and mAb sequences belonging to the same lineage as the ADI-67983 mAb. Sequences which remained after Fast Amplicon Denoising are marked in red. The tree is rooted on an inferred germline sequence obtained from the IgBLAST generated "germline_alignment" column of the sequence with the smallest IGHV SHM in the lineage. **(B)** IGHV SHM nucleotide percentage dot plots for the ADI-66175 and ADI-67983 clones IgG Rep-seq sequences, demonstrating the difference between SHM distributions with and without chimera removal. Blue crossbars are NGS data averages. **(C)** Sequence count data at each processing step. **(D)** Heatmap of clonally collapsed IGHV gene frequencies of bulk libraries and mAbs.

Supplementary Table 1 | Fig. 1 serum titer donor samples datasheet.

Supplementary Table 2 | IML3694 and IML3695 donor samples datasheet.

Supplementary Table 3 | Monoclonal antibody data sheet including sequence data, subdomain specificities, neutralization titers, and VDJ gene assignment.

Supplementary Table 4 | IgDiscover inferred genotypes for IML3694 and IML3695.

ACKNOWLEDGEMENTS

This project was supported by a grant from the SciLifeLab National COVID-19 Research Program (C19VE:G:007) to M.N.E.F and G.K.H and funded by the Knut and Alice Wallenberg Foundation, as well as a Distinguished Professor grant from the Swedish Research Council (2017-00968) to GKH and a project grant (2020-06235) to M.N.E.F. We would like to thank the study participants and Claes Ahlm, Johan Norberg and the Clinical Research Center, Norrlands University Hospital, Umeå for acquisition of serum samples analyzed in Supplementary Fig. 1. We gratefully acknowledge the G2P-UK National Virology consortium funded by MRC/UKRI (grant ref: MR/W005611/1.) and the Barclay Lab at Imperial College for providing spike expression plasmids. Open access funding provided by Karolinska Institutet. We also thank the Fondation Dormeur (Liechtenstein) for generous contribution towards equipment.

COMPETING INTERESTS

M.S., C.G.R. and H.L.D. are employees of Adimab LLC. and own equity stake in Adimab LLC. L.M.W. is an employee of Invivyd Inc. and owns shares in Invivyd Inc. The other authors declare no competing interests.

CORRESPONDENCE ABOUT MATERIALS

Questions about materials can be addressed to: Gunilla B. Karlsson Hedestam, E-mail: gunilla.karlsson.hedestam@ki.se and Laura Walker, Email: lwalker@invivyd.com

AUTHOR CONTRIBUTIONS

M.Ch., M.S., B.M., L.M.W. and G.B.K.H designed the study, analyzed the results, and wrote the manuscript. M.S. R.I.C, H.L.D. C.G.R. and M.F. selected the samples. D.S. and P.F.W. performed neutralization studies and M.C. generated the Rep-seq libraries and performed the personalized genotyping. A.S. implemented the chimera detection method. All authors revised the manuscript and approved the final version prior to submission.

REFERENCES

1. Castro Dopico, X., et al., *Probabilistic classification of anti-SARS-CoV-2 antibody responses improves seroprevalence estimates.* Clin Transl Immunology, 2022. **11**(3): p. e1379.
2. Shrock, E., et al., *Viral epitope profiling of COVID-19 patients reveals cross-reactivity and correlates of severity.* Science, 2020. **370**(6520).
3. Wang, Y., et al., *Kinetics of viral load and antibody response in relation to COVID-19 severity.* J Clin Invest, 2020. **130**(10): p. 5235-5244.
4. Gaebler, C., et al., *Evolution of antibody immunity to SARS-CoV-2.* Nature, 2021. **591**(7851): p. 639-644.
5. Muecksch, F., et al., *Affinity maturation of SARS-CoV-2 neutralizing antibodies confers potency, breadth, and resilience to viral escape mutations.* Immunity, 2021. **54**(8): p. 1853-1868 e7.
6. Sakharkar, M., et al., *Prolonged evolution of the human B cell response to SARS-CoV-2 infection.* Sci Immunol, 2021. **6**(56).
7. Baden, L.R., et al., *Efficacy and Safety of the mRNA-1273 SARS-CoV-2 Vaccine.* N Engl J Med, 2021. **384**(5): p. 403-416.
8. Polack, F.P., et al., *Safety and Efficacy of the BNT162b2 mRNA Covid-19 Vaccine.* N Engl J Med, 2020. **383**(27): p. 2603-2615.
9. Muecksch, F., et al., *Increased memory B cell potency and breadth after a SARS-CoV-2 mRNA boost.* Nature, 2022. **607**(7917): p. 128-134.
10. Tseng, H.F., et al., *Effectiveness of mRNA-1273 against SARS-CoV-2 Omicron and Delta variants.* Nat Med, 2022. **28**(5): p. 1063-1071.
11. Ebinger, J.E., et al., *Antibody responses to the BNT162b2 mRNA vaccine in individuals previously infected with SARS-CoV-2.* Nat Med, 2021. **27**(6): p. 981-984.
12. Goel, R.R., et al., *Distinct antibody and memory B cell responses in SARS-CoV-2 naive and recovered individuals following mRNA vaccination.* Sci Immunol, 2021. **6**(58).
13. Krammer, F., et al., *Antibody Responses in Seropositive Persons after a Single Dose of SARS-CoV-2 mRNA Vaccine.* N Engl J Med, 2021. **384**(14): p. 1372-1374.
14. Reynolds, C.J., et al., *Prior SARS-CoV-2 infection rescues B and T cell responses to variants after first vaccine dose.* Science, 2021.
15. Stamatatos, L., et al., *mRNA vaccination boosts cross-variant neutralizing antibodies elicited by SARS-CoV-2 infection.* Science, 2021.
16. Wang, Z., et al., *Naturally enhanced neutralizing breadth against SARS-CoV-2 one year after infection.* Nature, 2021. **595**(7867): p. 426-431.
17. Cele, S., et al., *Escape of SARS-CoV-2 501Y.V2 from neutralization by convalescent plasma.* Nature, 2021. **593**(7857): p. 142-146.
18. Garcia-Beltran, W.F., et al., *Multiple SARS-CoV-2 variants escape neutralization by vaccine-induced humoral immunity.* Cell, 2021. **184**(9): p. 2523.
19. Liu, J., et al., *BNT162b2-elicited neutralization of B.1.617 and other SARS-CoV-2 variants.* Nature, 2021. **596**(7871): p. 273-275.
20. Planas, D., et al., *Considerable escape of SARS-CoV-2 Omicron to antibody neutralization.* Nature, 2021.
21. Sheward, D.J., et al., *Neutralisation sensitivity of the SARS-CoV-2 omicron (B.1.1.529) variant: a cross-sectional study.* Lancet Infect Dis, 2022. **22**(6): p. 813-820.
22. Wang, P., et al., *Antibody resistance of SARS-CoV-2 variants B.1.351 and B.1.1.7.* Nature, 2021. **593**(7857): p. 130-135.
23. Zost, S.J., et al., *Rapid isolation and profiling of a diverse panel of human monoclonal antibodies targeting the SARS-CoV-2 spike protein.* Nat Med, 2020. **26**(9): p. 1422-1427.
24. Corcoran, M.M., et al., *Production of individualized V gene databases reveals high levels of immunoglobulin genetic diversity.* Nat Commun, 2016. **7**: p. 13642.
25. Barnes, C.O., et al., *SARS-CoV-2 neutralizing antibody structures inform therapeutic strategies.* Nature, 2020. **588**(7839): p. 682-687.
26. Tan, T.J.C., et al., *Sequence signatures of two public antibody clonotypes that bind SARS-CoV-2 receptor binding domain.* Nat Commun, 2021. **12**(1): p. 3815.

27. Vanshylla, K., et al., *Discovery of ultrapotent broadly neutralizing antibodies from SARS-CoV-2 elite neutralizers.* Cell Host Microbe, 2022. **30**(1): p. 69-82 e10.
28. Yuan, M., et al., *Structural basis of a shared antibody response to SARS-CoV-2.* Science, 2020. **369**(6507): p. 1119-1123.
29. Yuan, M., et al., *Recognition of the SARS-CoV-2 receptor binding domain by neutralizing antibodies.* Biochem Biophys Res Commun, 2021. **538**: p. 192-203.
30. Kumar, V., et al., *Long-read amplicon denoising.* Nucleic Acids Res, 2019. **47**(18): p. e104.
31. Song, G., et al., *Cross-reactive serum and memory B-cell responses to spike protein in SARS-CoV-2 and endemic coronavirus infection.* Nat Commun, 2021. **12**(1): p. 2938.
32. Tegally, H., et al., *Emergence of SARS-CoV-2 Omicron lineages BA.4 and BA.5 in South Africa.* Nat Med, 2022.
33. Cao, Y., et al., *Omicron escapes the majority of existing SARS-CoV-2 neutralizing antibodies.* Nature, 2022. **602**(7898): p. 657-663.
34. Wang, Q., et al., *Antibody evasion by SARS-CoV-2 Omicron subvariants BA.2.12.1, BA.4 and BA.5.* Nature, 2022. **608**(7923): p. 603-608.
35. Ng, K.W., et al., *Preexisting and de novo humoral immunity to SARS-CoV-2 in humans.* Science, 2020. **370**(6522): p. 1339-1343.
36. Hurlburt, N.K., et al., *Structural definition of a pan-sarbecovirus neutralizing epitope on the spike S2 subunit.* Commun Biol, 2022. **5**(1): p. 342.
37. Sundling, C., et al., *Soluble HIV-1 Env trimers in adjuvant elicit potent and diverse functional B cell responses in primates.* J Exp Med, 2010. **207**(9): p. 2003-17.
38. Wrammert, J., et al., *Rapid cloning of high-affinity human monoclonal antibodies against influenza virus.* Nature, 2008. **453**(7195): p. 667-71.
39. Hoehn, K.B., et al., *Human B cell lineages associated with germinal centers following influenza vaccination are measurably evolving.* Elife, 2021. **10**.
40. Poon, M.M.L., et al., *SARS-CoV-2 infection generates tissue-localized immunological memory in humans.* Sci Immunol, 2021. **6**(65): p. eabl9105.
41. Mesin, L., et al., *Restricted Clonality and Limited Germinal Center Reentry Characterize Memory B Cell Reactivation by Boosting.* Cell, 2020. **180**(1): p. 92-106 e11.
42. Tan, H.X., et al., *Lung-resident memory B cells established after pulmonary influenza infection display distinct transcriptional and phenotypic profiles.* Sci Immunol, 2022. **7**(67): p. eabf5314.
43. MacLean, A.J., et al., *Secondary influenza challenge triggers resident memory B cell migration and rapid relocation to boost antibody secretion at infected sites.* Immunity, 2022. **55**(4): p. 718-733 e8.
44. Gietz, R.D. and R.A. Woods, *Transformation of yeast by lithium acetate/single-stranded carrier DNA/polyethylene glycol method.* Methods Enzymol, 2002. **350**: p. 87-96.
45. Wec, A.Z., et al., *Broad neutralization of SARS-related viruses by human monoclonal antibodies.* Science, 2020. **369**(6504): p. 731-736.
46. Rogers, T.F., et al., *Isolation of potent SARS-CoV-2 neutralizing antibodies and protection from disease in a small animal model.* Science, 2020. **369**(6506): p. 956-963.
47. Stoler, N. and A. Nekrutenko, *Sequencing error profiles of Illumina sequencing instruments.* NAR Genom Bioinform, 2021. **3**(1): p. lqab019.
48. Phad, G.E., et al., *Extensive dissemination and intraclonal maturation of HIV Env vaccine-induced B cell responses.* J Exp Med, 2020. **217**(2).
49. Katoh, K., et al., *MAFFT: a novel method for rapid multiple sequence alignment based on fast Fourier transform.* Nucleic Acids Res, 2002. **30**(14): p. 3059-66.
50. Price, M.N., P.S. Dehal, and A.P. Arkin, *FastTree: computing large minimum evolution trees with profiles instead of a distance matrix.* Mol Biol Evol, 2009. **26**(7): p. 1641-50.
51. Yu, G., et al., *Two Methods for Mapping and Visualizing Associated Data on Phylogeny Using Ggtree.* Mol Biol Evol, 2018. **35**(12): p. 3041-3043.

Figures

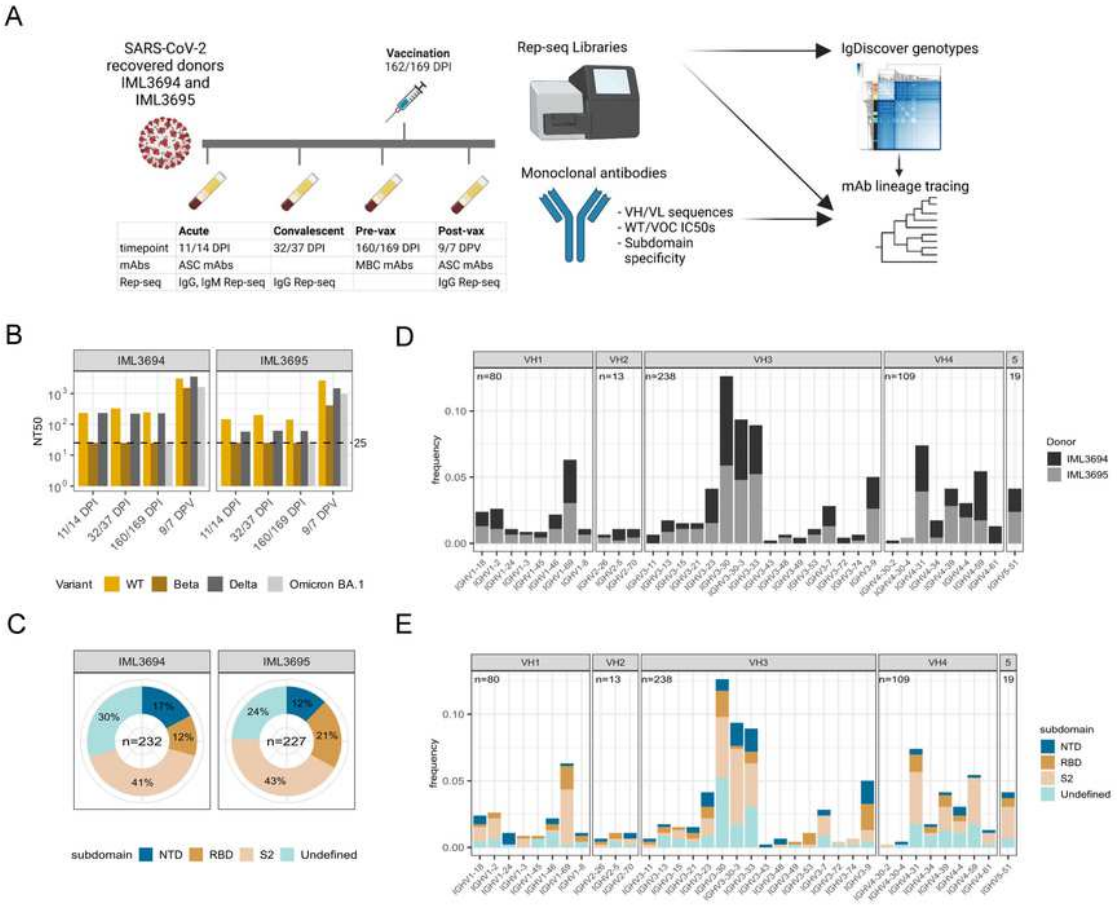

FIG. 1 | Study design, serum neutralizing activity and properties of spike-binding monoclonal antibodies (mAbs). **(A)** Schematic of study design with time points for infection and vaccination, mAb isolation, and samples for NGS. **(B)** IML3694 and IML3695's serum neutralizing antibody values against ancestral SARS-CoV-2 Wuhan (WT) and variants of concern (VOCs). **(C)** Pie chart of mAb subdomain specificities in the two donors. **(D)** mAb IGHV allele frequencies colored by donor. **(E)** mAb IGHV allele frequencies colored by subdomain specificity.

Figure 1

Figure 1

See above image for figure legend.

Donor	mAb ID	VH gene	JH gene	HCDR3	% VH SHM nt	VL gene	JL gene	LCDR3	% VL SHM nt	WT IC50 (µg/ml)	Beta IC50 (µg/ml)	Delta IC50 (µg/ml)	Omicron BA.1 IC50 (µg/ml)	Omicron BA.2.75 IC50 (µg/ml)	Omicron BA.5 IC50 (µg/ml)
IML3694	ADI-67481	IGHV3-53*02	IGHJ4*02	ARDLDVMGGFDY	2	IGKV1-9*01	IGKJ1*01	QELNSYPRT	2.1	0.0589	>1	0.1227	N.D.	N.D.	N.D.
IML3694	ADI-67485	IGHV1-69*01	IGHJ2*01	ATGVRYCDTTSCRASYFDF	4.7	IGKV3-20*01	IGKJ2*01	QQYGSSPLT	1.7	0.0148	N.D.	0.2704	4.211	N.D.	N.D.
IML3694	ADI-67649	IGHV4-4*02	IGHJ4*02	ARDIRQDDCSTTRCPEY	5.1	IGKV3-11*01	IGKJ3*01	QQRSNWPPT	1.7	0.012	>1	0.0302	N.D.	N.D.	N.D.
IML3694	ADI-67652	IGHV1-2*02	IGHJ6*03	ARDRNWAIFGVESDV	5.7	IGLV2-23*02	IGLJ3*02	CSYADSSAWV	4.1	0.1698	>1	0.302	N.D.	N.D.	N.D.
IML3694	ADI-67657	IGHV3-23*01	IGHJ4*02	AKDRLRTSSLQPMPFFDY	3.7	IGKV4-1*01	IGKJ1*01	QQYYSAPYT	1.7	0.0081	N.D.	>1	2.139	N.D.	N.D.
IML3694	ADI-67679	IGHV3-53*02	IGHJ4*02	ARDLAGPGLFDH	5.8	IGKV1-33*01	IGKJ5*01	QQYDNVPSIT	3.2	0.0584	>1	0.0599	0.1204	N.D.	N.D.
IML3694	ADI-67680	IGHV3-33*01	IGHJ2*01	ARDGTIAVAGTFDRFFDL	3.4	IGKV1-33*01	IGKJ3*01	QQYHILPFT	3.9	0.1108	>1	0.2379	N.D.	N.D.	N.D.
IML3694	ADI-67722	IGHV4-34*01	IGHJ6*03	ARGVQIPEYCSMNNCPVSDHHYFYMDV	13.3	IGKV3-20*01	IGKJ1*01	QQYGGSRPWT	4.5	0.0282	0.2552	0.0122	N.D.	N.D.	N.D.
IML3694	ADI-67726	IGHV1-8*01	IGHJ6*03	ATKRVQVPRRYYYYMDL	3.1	IGKV2-28*01	IGKJ4*01	MQSLQTPLT	2	0.0258	N.D.	0.0235	N.D.	N.D.	N.D.
IML3694	ADI-67744	IGHV3-9*01	IGHJ6*02	AKGKAAGHSYYYGMDV	3.4	IGKV1-39*01	IGKJ1*01	QQSYVTPWT	3.9	0.0154	0.0272	0.0102	0.01366	0.007	>1
IML3694	ADI-67748	IGHV4-31*03	IGHJ4*02	ARSPVIYGTNSGFDY	5.7	IGKV5-2*01	IGKJ1*01	LQHDNFPYT	1.1	0.0082	0.0322	0.0431	4.405	N.D.	N.D.
IML3694	ADI-67757	IGHV1-8*01	IGHJ6*02	ARGNYFDGDGYVDY	4.1	IGKV3-15*01	IGKJ4*01	QQYNNWPLT	3.2	0.0216	N.D.	0.0302	N.D.	N.D.	N.D.
IML3694	ADI-67831	IGHV3-49*03	IGHJ4*02	TLTVTNRYYFHS	2.4	IGKV3-15*01	IGKJ2*03	QQYNNWFS	0.7	0.009	>1	0.8322	N.D.	N.D.	N.D.
IML3695	ADI-67119	IGHV3-53*02	IGHJ6*02	ARDSVRGGMDV	5.8	IGLV3-9*01	IGLJ2*01	QVWDTTSVI	8.6	0.065	0.6351	0.0808	N.D.	N.D.	N.D.
IML3695	ADI-67127	IGHV3-9*01	IGHJ3*02	AKDDYPSSWYEHHPQRWAFDI	3.7	IGLV1-51*01	IGLJ3*02	GTWDSSLSVV	0.3	0.0541	>1	>1	N.D.	N.D.	N.D.
IML3695	ADI-67135	IGHV3-9*01	IGHJ4*02	AKGGEYSSRWYLRESYFDY	5.1	IGKV2D-29*01	IGKJ4*01	MQSIQVPLT	1.7	0.0025	N.D.	>1	N.D.	N.D.	N.D.
IML3695	ADI-67138	IGHV4-39*01	IGHJ4*02	AVGGVRSLEWLLQFDY	6.1	IGLV2-8*01	IGLJ1*01	SSYAGSSSLV	2.7	0.0085	0.001	0.003	0.002276	0.003	>1
IML3695	ADI-67139	IGHV4-31*03	IGHJ4*02	ARDSDYGEYFDS	3.3	IGKV3-11*01	IGKJ5*01	QQRYNWPPIT	1.7	0.2125	>1	>1	N.D.	N.D.	N.D.
IML3695	ADI-67140	IGHV3-53*02	IGHJ3*02	AREAYAFDI	5.5	IGKV1-9*01	IGKJ4*01	QQLNSHPPA	2.1	0.012	>1	0.015	N.D.	N.D.	N.D.
IML3695	ADI-67183	IGHV4-39*01	IGHJ4*02	AVGGVRFFEWLLQFDY	3.7	IGLV2-8*01	IGLJ2*01	SSYAGSSSLI	3.7	0.0029	0.0027	0.0008	0.003034	0.005	>1
IML3695	ADI-67189	IGHV3-30*03	IGHJ4*02	ARDYGDYAAFDS	4.4	IGKV4-1*01	IGKJ4*01	QQYYSTPLT	1.3	0.2776	>1	>1	N.D.	N.D.	N.D.
IML3695	ADI-67218	IGHV4-34*01	IGHJ3*02	ARWDLLYPRDAFDI	3.1	IGLV2-11*01	IGLJ2*01	CSYAGSYVV	2.1	0.0657	>1	0.057	N.D.	N.D.	N.D.
IML3695	ADI-67852	IGHV3-9*01	IGHJ4*02	AKDIQFRDRDCTNGVCSVGGFDY	5.7	IGKV3-15*01	IGKJ2*01	QQYNKWPPRT	1.7	0.2345	>1	>1	1.103	N.D.	N.D.
IML3695	ADI-67857	IGHV4-39*01	IGHJ4*02	AVGGVRFLEWLLQFDY	2.4	IGLV2-8*01	IGLJ1*01	SSYAGSSNLV	1.7	0.0027	0.0727	0.0159	0.01917	0.089	>1
IML3695	ADI-67935	IGHV4-31*03	IGHJ4*02	ARGPYASGSFDS	5	IGKV3-20*01	IGKJ1*01	HHYGSSGDT	2.1	0.048	N.D.	0.039	N.D.	N.D.	N.D.
IML3695	ADI-67971	IGHV3-9*01	IGHJ3*02	AKLGGAN.D.YDFRSGPTAFDI	4.4	IGLV1-44*01	IGLJ2*01	ATWDDSLNGVVV	2	0.1363	0.3985	>1	0.1333	N.D.	N.D.
IML3695	ADI-67977	IGHV3-9*01	IGHJ6*02	VKDMSVGDRSVEYYGMDV	2	IGLV3-21*04	IGLJ2*01	QVWDSSSENVV	2.1	0.0759	0.2904	0.4427	0.02833	N.D.	N.D.
IML3695	ADI-67981	IGHV1-69*01	IGHJ3*02	ARDGRHNYDSTGYYHN.D.FDI	5.7	IGKV1-39*01	IGKJ1*01	QQSYSSRT	3.2	0.0094	>1	0.0117	0.04438	N.D.	N.D.
IML3695	ADI-67983	IGHV3-9*01	IGHJ4*02	AKGKWPSSPSFLTDY	5	IGKV1-27*01	IGKJ4*01	QKYNSVPLT	3.5	0.0031	>1	0.0049	N.D.	N.D.	N.D.
IML3695	ADI-67994	IGHV3-23*01	IGHJ6*02	ARDLGGYSYGLNFFYAMDV	3.8	IGLV2-14*03	IGLJ2*01	SSYTSSSTFVL	2	0.1967	0.3379	0.227	0.3084	N.D.	N.D.
IML3695	ADI-67999	IGHV1-69*01	IGHJ4*02	ARERGYSGYGASLYFDY	5.1	IGLV1-40*01	IGLJ1*01	QSYDSSLSGAV	1.7	0.5019	0.6414	>1	0.1381	N.D.	N.D.

FIG. 2 | A summary of all neutralizing mAbs with an IC_{50} below 0.4 mg/ml against any of the SARS-CoV-2 VOCs.

Figure 2

Figure 2

See above image for figure legend.

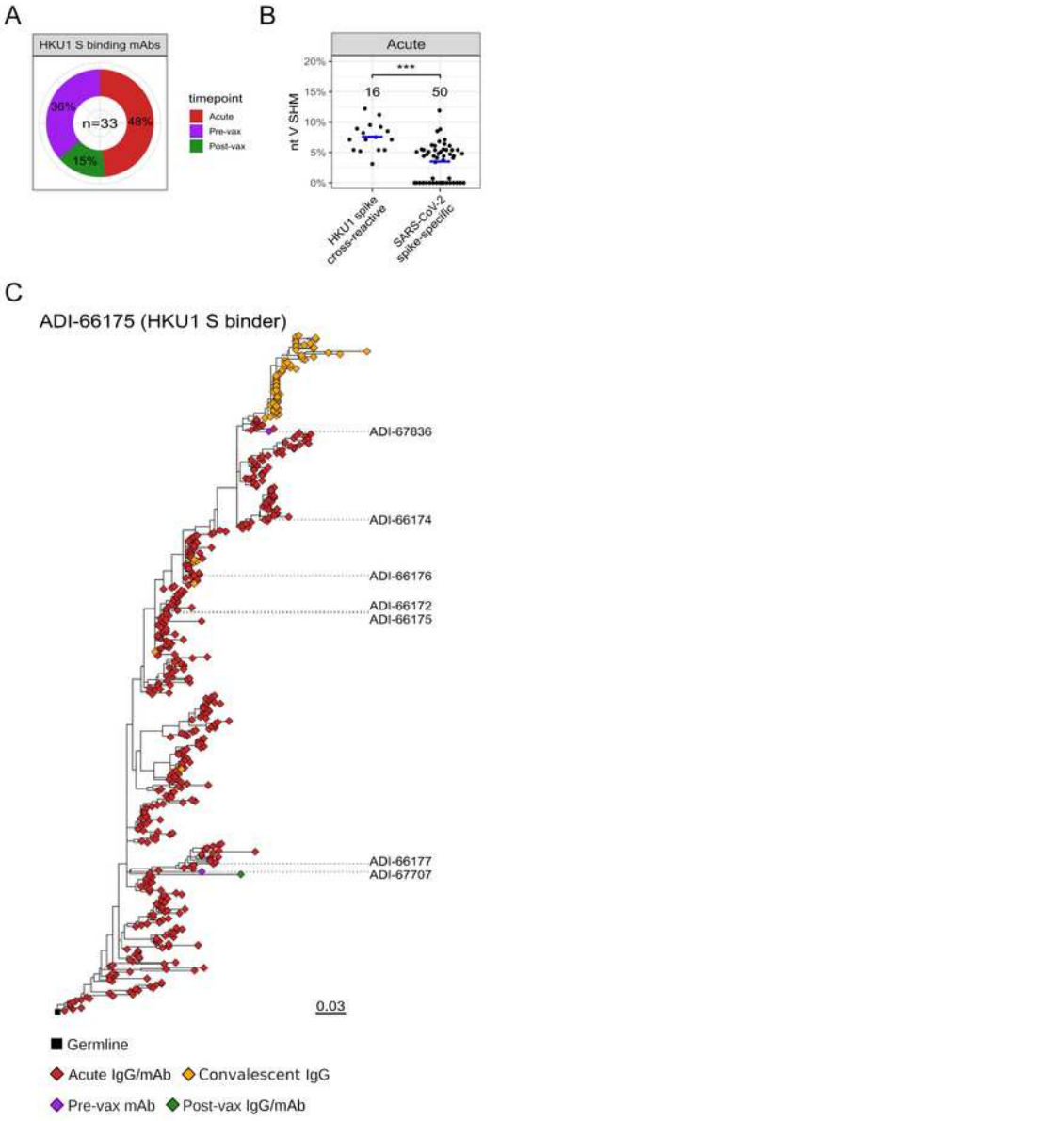

FIG. 3 | Isolation time point and evolution of HCoV-HKU1 S cross-reactive mAbs. **(A)** Pie chart of timepoints in which HCoV-HKU1 S-binding mAbs were isolated. **(B)** Dot plot of % nucleotide IGHV SHM for the HCoV-HKU1 S cross-reactive and SARS-CoV-2 S-specific mAbs isolated at the acute timepoint. Mann-Whitney U test used for comparison. **(C)** Maximum likelihood phylogenetic trees of HCoV-HKU1 S-binding traced lineage ADI-66175. The germline sequence was obtained from the IgBLAST generated "germline_alignment" column of the sequence with the minimum IGHV SHM in the lineage.

Figure 3

Figure 3

See above image for figure legend.

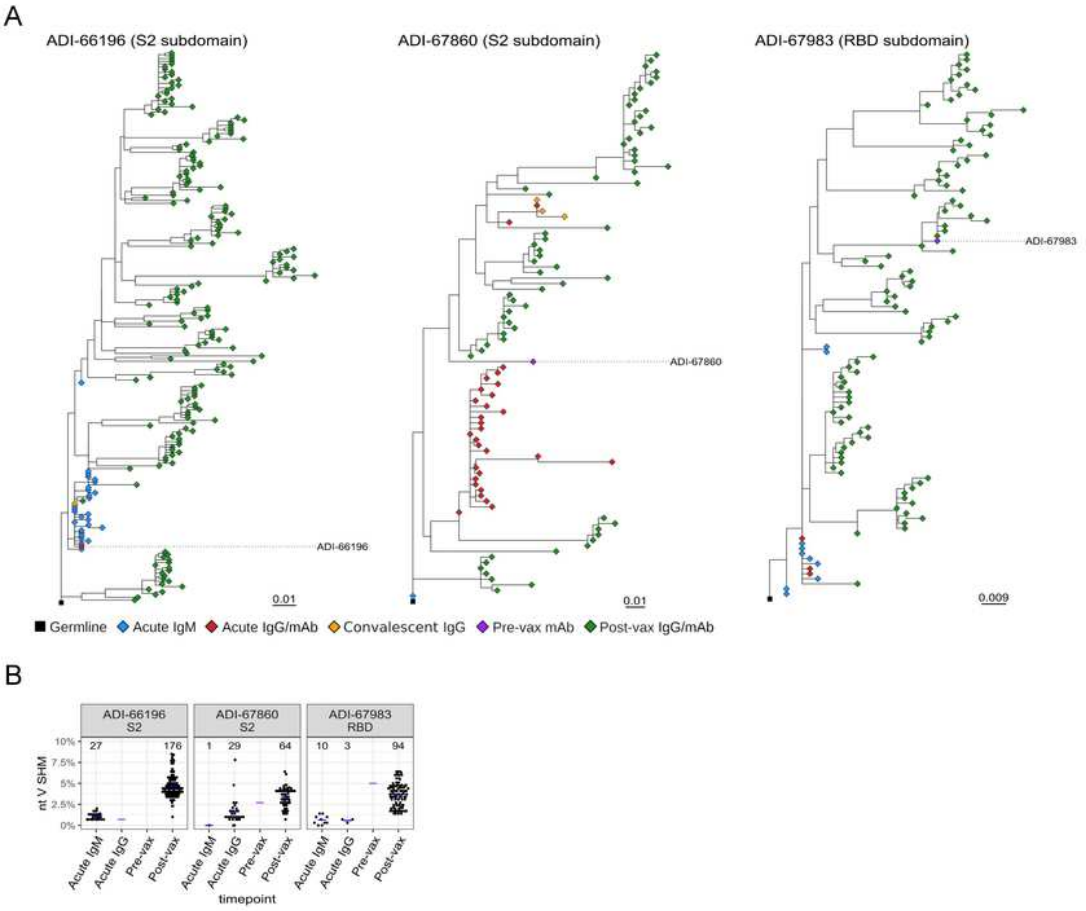

FIG. 4 | Evolution of SARS-CoV-2 S-specific antibody lineages over the sampling time points. **(A)** Maximum likelihood phylogenetic trees of traced lineages containing IgM Rep-seq sequences: ADI-66196, ADI-67860, and ADI-67983. Germlines sequences were obtained from the IgBLAST generated "germline_alignment" column of the sequence with the smallest IGHV SHM in the lineage. **(B)** Dot plot of % nucleotide IGHV SHM for the ADI-66196, ADI-67860, and ADI-67983 lineage sequences. Purple crossbars represent mAb values, while the blue crossbars represent average values of traced variants for each timepoint.

Figure 4

Figure 4

See above image for figure legend.

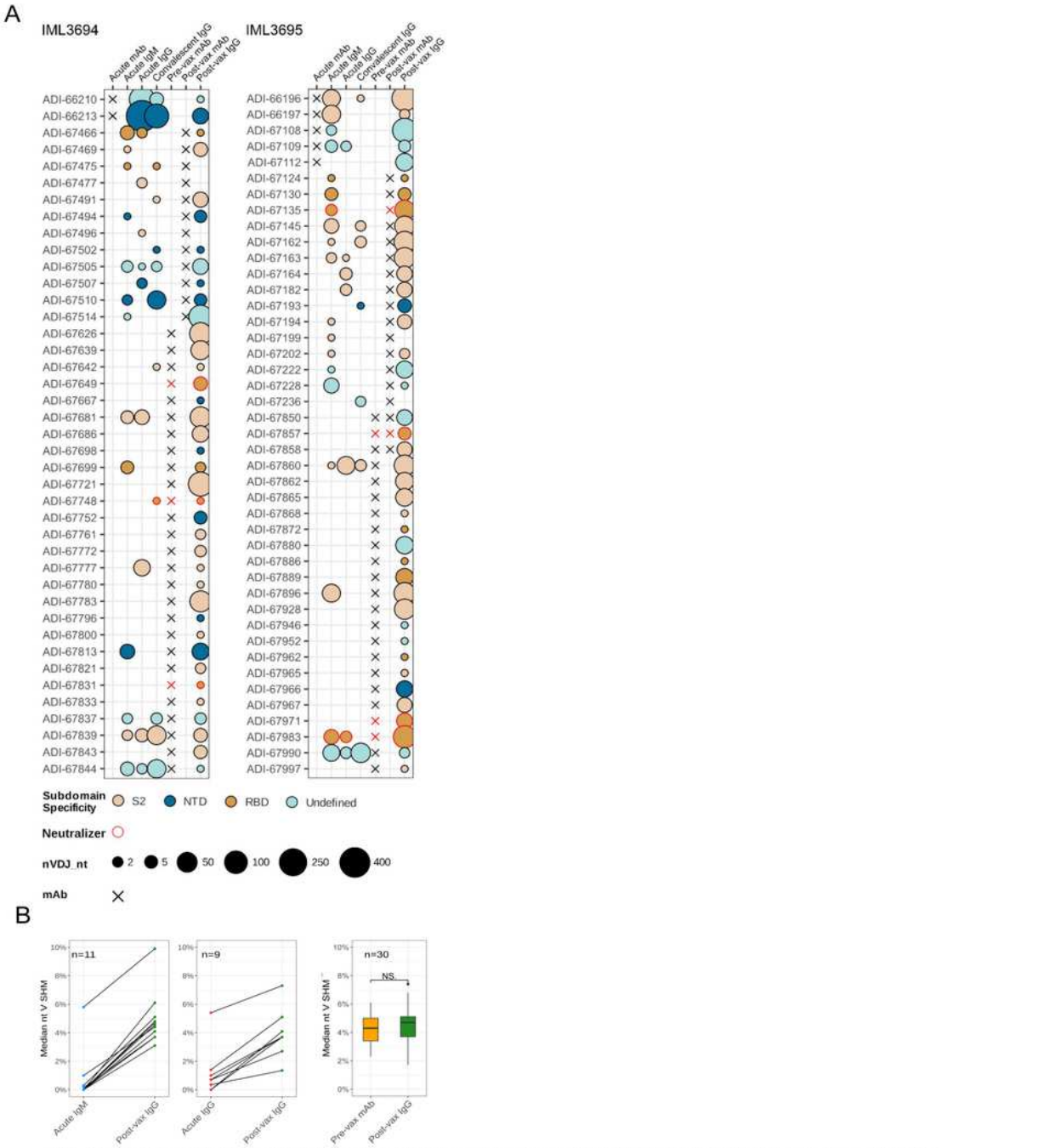

FIG. 5 | IgM and IgG repertoire sequencing and lineage tracing of SARS-CoV-2 S-specific antibody lineages at the longitudinal time points. **(A)** Bubble plots of SARS-CoV-2 S-specific mAb lineages found before and after vaccination in IML3694 and IML3695. The bubble sizes correspond to post-FAD and chimera cleaned data. **(B)** Line plots of median % nucleotide IGHV SHM for lineages found in acute IgM/IgG and post-vax IgG Rep-seq data. **(C)** Boxplot of median % nucleotide IGHV SHM for lineages containing pre-vax timepoint mAbs and post-vax IgG Rep-seq. Wilcoxon signed-rank test used for comparison.

Figure 5

Figure 5

See above image for figure legend.

Supplementary Files

This is a list of supplementary files associated with this preprint. Click to download.

- Chernyshev.etal.figures.pdf
- Supplementarytable1.xlsx
- Supplementarytable2.xlsx
- Supplementarytable3.xlsx
- Supplementarytable4.xlsx
- nrreportingsummary.pdf